Modeling and Simulation of the Maximum Power Point Tracking Control by Fuzzy Logic: Application to The Photovoltaic Energy Potential of the Cities of Fada, Doba and Amdjaras in Chad

Kalmobe Pallai, Mbainaibeye Jerome, Kamta Martin, Tom Cherif Bilio

***Abstract*— This article presents the modeling of the photovoltaic generator connected to the electrical network under a hot climate. A collection of meteorological data was made on the ground in AMDJARAS, Doba and Fada on the one hand and on the other hand through the NASA meteorological database. These data made it possible to estimate the photovoltaic and wind energy resources available in the three cities of Chad. The solar irradiance data collected made it possible to identify favorable areas for the installation of a photovoltaic (PV) power plant among the three chosen cities. The use of this database shows that the cities of AMDJARASS and FADA are very favorable to a photovoltaic installation. However, the PV voltage are variable over the course of the sun. At first, we searched for the maximum power to be extracted through the intelligent Maximum Power Point Tracking (MPPT) control based on fuzzy logic and the Pertub and Observ (P&O) technique. In second step, we studied the stability of the voltage at the output using a non-inverting buck-boost chopper. For voltage stability, the results obtained are satisfactory for a variation of solar irradiance from 1000W/m^2 to 500W/m^2. The contribution of this work is in the one hand the modeling of the photovoltaic generator connected to the network under a hot climate, the reaching of the maxim voltage by an intelligent using of MPPT based on the fuzzy logic algorithms. the stability of the output voltage is obtained by the using of a non-inverting buck-boost chopper.**

***Index Terms*— Buck-boost chopper, Hot climate, MPPT control,Neuro-fuzzy, photovoltaic generator modeling.**

I. INTRODUCTION

Energy is a vital source for global socio-economic development, growth in average global primary energy consumption is estimated at 1.5% over the last decade [1], while fossil resources are the main source of supply in energy. This source of energy contributes to the increase of greenhouse gases and significantly harms the environment. It is everyone's duty to modify this practice in order to align with the policy of international summits (cop21, cop22, cop27, etc.) for the protection of the environment.

The Sahelian zone has an enormous solar energy resource estimated at 4.5 to 6.5 kWh/m^2/day [2]. In Chad, the government priority is more based on the exploitation of fossil fuels. However, given the global context of climate change visible today with its batches of floods and droughts, the government is obliged to redirect the production of electricity based on renewable energy resources. The work presented in this article aims initially to assess the photovoltaic solar energy potential in the cities of Doba, Amdjarass and Fada by collecting data. In a second step, make a theoretical and semi-experimental study of the photovoltaic system and the Maximum Power Point Tracking (MPPT) control. Finally, in a third step, seek the stability of the voltage at the output of the system. The rest of the paper is organized as follows: Section 2 presents the state of the art in connected solar photovoltaic systems. Section 3 presents the measurements of the photovoltaic energy deposits of three localities in Chad by the data which we have collected. Section 4 describes the different diagrams and equations for modeling the photovoltaic conversion chain that we have developed for its implementation and evaluation. The modeling as well as the search for the maximum power point are presented by section 5. Section 6 presents the results as well as the discussions. Finally, section 7 presents the conclusion and perspectives of this work.

II. STATE OF THE ART ON GRID-CONNECTED PV SYSTEM

For ecological and economic development, the coupling of an MPPT system to the Grid connected Photo-voltaic system (GPV) is favorable (see Fig. 1) [3]. This system

therefore consists of a PV generator stage with its MPPT system and a three-phase inverter with a DC bus upstream.

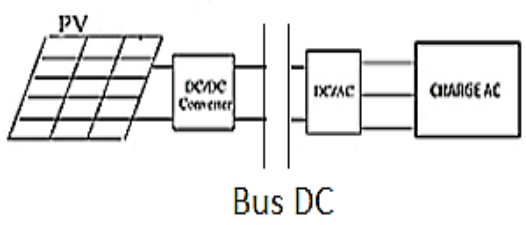

Fig. 1 Grid-connected PV system

The advantage of choosing such a GPV+MPPT coupling in the Sahelian zone is to have more energy at the output but the risk is to have too much solar irradiance in a certain locality and not in another.

A. ESTIMATION OF PV ENERGY DEPOSITS

A.1. ESTIMATION OF SOLAR DEPOSIT

The global solar irradiance on an inclined plane is calculated by the Eq. (1) [4]:

$$G_{inc} = B_{in} + D_i + R_i \quad (1)$$

Where Bin is the direct irradiation, Di the diffuse irradiance and Ri the irradiation reflected on an inclined plane.

A.2. MONTHLY AVERAGE OF THE DIRECT IRRADIATION B_{in} ON THE INCLINED PLANE

The direct irradiation on the inclined plane is estimated by the following relationship Eq.(2):

$$B_{in} = R_b(G_H - D_H) \quad (2)$$

With, G_H, D_H, and R_b respectively the hourly values of the global, diffuse and form factor irradiations. This is given by the Eq. (3):

$$R_b = cos(\theta_i)/sin(h) \quad (3)$$

Where Θ_i and h are respectively the angle of incidence and the height of the sun.

A.3. MONTHLY AVERAGE OF THE DIFFUSE IRRADIATION D_i ON THE INCLINED PLANE

The diffuse monthly irradiation on any inclined plane is given by the Eq. (4):

$$D_i = D_H \left(\frac{1-cos(\beta)}{2}\right) \quad (4)$$

With β the angle of inclination of the capture surface and D_H the diffuse irradiation on the horizontal plane.

A.4. MONTHLY AVERAGE OF THE REFLECTED IRRADIATION R_i ON THE INCLINED PLANE

The estimate of the average irradiation reflected by the ground and incident on any plane is given by the Eq. (5):

$$R_i = (B_m sin(h) + D_H)\rho \left(\frac{1-cos(\beta)}{2}\right) \quad (5)$$

With ρ and Bn are respectively the albedo of the ground and the direct irradiation on a normal plane.

B. THE PV SYSTEM

The PV conversion and PV energy adaptation chain are described by the following set of interconnected systems in Fig. 2:

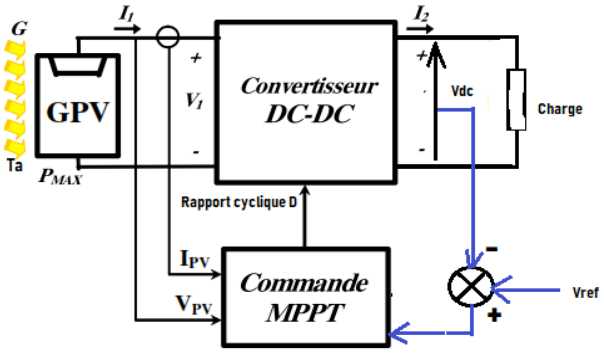

Fig. 2 PV power regulation system

The principle of operation of the MPPT control consists in measuring the voltage and the current at the output of the PV generator, then delivering a signal allowing to excite an electronic switch of the DC-DC converter in order to maintain the point of maximum power of the characteristic of the PV generator at any time [5, 6, 10].

III. MEASUREMENTS OF PV ENERGY DEPOSITS IN THREE LOCALITIES IN CHAD

We measured the photovoltaic energy deposits by collecting solar irradiance data at 2 meters from the ground and temperature at 10 meters from the ground for 30 years (from 1989 to 2019) that we carried out in the cities of AMDJARAS, DOBA and FADA. These data are from NASA. The corresponding geographical coordinates are: latitude 16.19 and longitude 22.27 for AMDJARAS; latitude 8.0 and longitude 16.0 for DOBA and finally latitude 17.19 and longitude 21.58 for FADA. Fig. 3 to Fig. 6 show the results of the data collected in the three above cities.

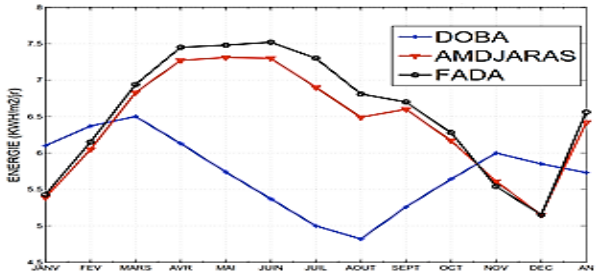

Fig. 3 average solar irradiance at 2m from the ground for 30 years (1989-2019)

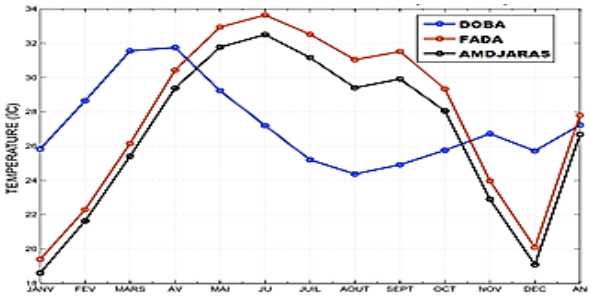

Fig. 4 Average temperature at 2m from the ground in the shade for 30 years (1989-2019)

The results (Fig. 3) show that the city of FADA is very favorable for the exploitation of PV solar energies with an annual average reaching 6.56 Kwh/m^2/day followed by the city of AMDJARAS (6.42 Kwh/m^2/day). The city of Doba has a low solar energy potential (5.73 Kwh/m^2/day) compared to the two previous cities.

Moreover, FADA is also the hottest city with an annual average of 27.79°C compared to the two other cities chosen, then the average temperature is 27.23°C in DOBA and 26.67°C in AMDJARASS (Fig. 4). Temperature is a factor that negatively affects the performance of PV generators. The comparison of experimental temperatures and those of NASA in the geographical location of coordinates of latitude 16.19, longitude 22.27 and altitude 752.23m and is shown in Fig. 5.

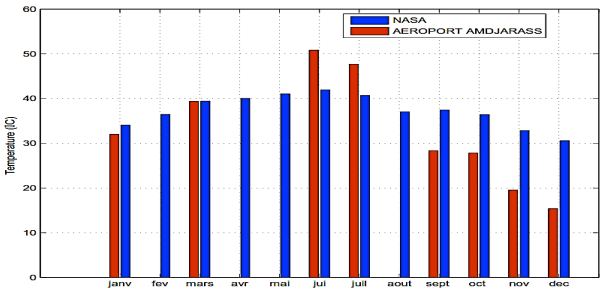

Fig.5 Comparison of monthly average maximum temperatures for the year 2019 between NASA source and AMDJARAS Airport

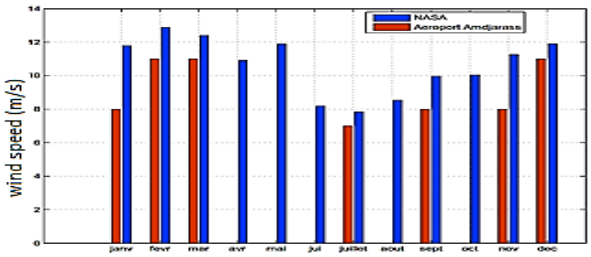

Fig. 6 Comparison of monthly average maximum speeds for the year 2019 between NASA source and AMDJARAS Airport

We find that the values of wind speeds and temperatures taken from the NASA databases are approximately the same as the experimental values measured at AMDJARAS Airport (Fig. 6).

IV. PV CONVERSION CHAIN

The PV cell is a PN junction semiconductor, so it can be modeled by a current source mounted in parallel with a diode (Fig. 7).

The current source generates a current I_{ph} proportional to the solar irradiance.

The current voltage relation at the output of the PV generator is given by Eq. (6), Eq. (7), and Eq. (8):

$$V_{pv} = \frac{nKT}{q}\ln\left(\frac{I_{ph}}{I_{pv}} + 1\right) \quad (6)$$

$$I_{pv} = I_{ph} - I_s\left[\exp\left(\frac{q\left(V_{pv}+I_{pv}R_s\right)}{nKT}\right) - 1\right] - \frac{V_{pv}+R_sI_{ph}}{R_{sh}} \quad (7)$$

$$V_T = \frac{KT}{q} \quad (8)$$

Where R_{sh} is the schunt resistance, R_s the serie resistance, I_{ph} the photo-generated current which depends on the solar irradiance, the surface S of the PV generator and the temperature T, I_S is the saturation current of the diode, n the ideality factor of the diode, K is the Boltzmann constant ($1.38\text{x}10^{-23}$J/K), q is the electronic charge, V_T the thermal potential which is a function of the temperature. The current I_{pv} is a nonlinear function which depends on the output voltage V_{pv}, the irradiance and the temperature T.

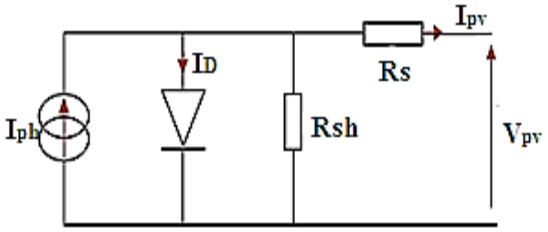

Fig. 7 Equivalent circuit of a photovoltaic cell

A. PINCIPLE OF FINDING THE MAXIMUM POWER POINT

The output voltage-power characteristics of a PV cell present a point for which the PV cell delivers the maximum possible power to the load for a well-defined climatic condition. The power in function of voltage and the current in function of voltage, together depending of the illuminance are presented respectively in Fig. 8 and Fig. 9.

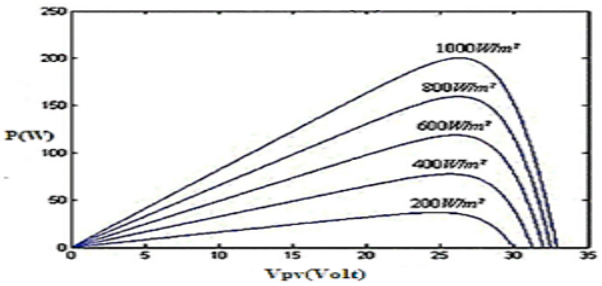

Fig. 8 Example of power/voltage characteristic network for different illuminances

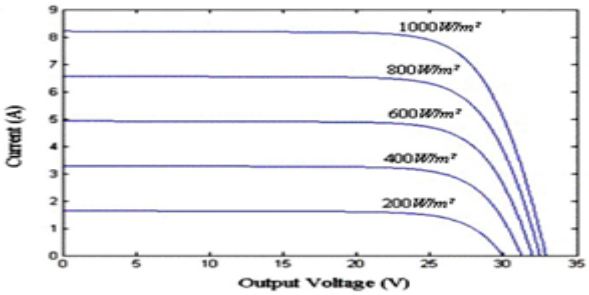

Fig. 9 Example of current/voltage characteristic network for different illuminances

The MPPT technique will cause the cell to operate very close to the Maximum Power Point (MPP) thanks to an impedance adapter controllable by a MPPT algorithm.

There are several MPPT algorithms used to drive the DC/DC converter such as Perturb and Observe (P&O) method, conductance increment method, gradient method, and smart fuzzy logic method.

B. PRINCIPLE OF THE BOOST CHOPPER

The chopper or DC-DC converter (Fig.10) is a power electronics device which allows the value of the voltage of a DC voltage source to be modified. If the output voltage is lower than the input voltage, the chopper is said to be buck, otherwise it is called a booster.

However, the buck-boost chopper combines the properties of the buck and boost configurations. It is used to transform any input voltage value into any output voltage value [3, 7, 12].

During operation of the chopper, the electronic switch is kept closed for a time αT, then open for a time (1-α) T, with α the duty cycle and T the switching period.

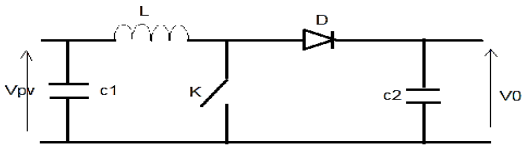

Fig. 10 Diagram of the booster chopper

- During the closing time of the electronic switch, the functionality of the electrical circuit is described by Eq. (9):

$$\begin{cases} i_{C1} = C_1 \frac{dv_{pv}}{dt} = i_{pv} - i_L \\ i_{C2} = C_2 \frac{dv_0}{dt} = -i_0 \\ v_L = L \frac{di_L}{dt} = v_{pv} - R_L i_L \end{cases} \quad (9)$$

- During the opening time interval of *K,* the functionality of the electrical circuit is described by Eq. (10):

$$\begin{cases} i_{C1} = C_1 \frac{dv_{pv}}{dt} = i_{pv} - i_L \\ i_{C2} = C_2 \frac{dv_0}{dt} = i_L - i_0 \\ v_L = L \frac{di_L}{dt} = v_{pv} - v_0 - R_L i_L \end{cases} \quad (10)$$

To find the dynamic expressions valid for a whole period *T*, we use the integral method over a following period *T* described by Eq. (11):

$$\frac{dX}{dt}.T = \alpha T \frac{dX}{dt_\alpha} + \frac{dX}{dt_{1-\alpha}} (1-\alpha)T$$

The application of this integral method over the two previous operating periods of the chopper leads to the Eq. (12):

$$\begin{cases} C_1 \frac{dv_{pv}}{dt}.T = \alpha T\left(i_{pv} - i_L\right) + (1-\alpha T)\left(i_{pv} - i_L\right) \\ C_2 \frac{dv_0}{dt} = -\alpha T i_0 + (1-\alpha T)(i_L - i_0) \\ L \frac{di_L}{dt} = \alpha T(v_{pv} - R_L i_L)(1-\alpha T)(v_{pv} - v_0 - R_L i_L) \end{cases} \quad (12)$$

In continuous mode, the derivative of the input and output quantities are all zero, and the time variables are replaced by their average value. In this case, Eq. (12) becomes:

$$\begin{cases} I_{pv} = I_L \\ I_0 = (1-\alpha) I_{pv} \\ V_0 = \frac{V_{pv}}{(1-\alpha)} \quad avec\ R_L \approx 0 \end{cases} \quad (13)$$

$$R_{Pv} = R_0 (1-\alpha)^2 \quad (14)$$

From Eq. (14), we determine the expression of α which is given by Eq. (15).

$$\alpha = 1 - \sqrt{\frac{R_{pv}}{R_0}} \quad (15)$$

Since the duty cycle is less than 1 (α < 1), the converter does not act as a voltage booster if $R_0 > R_{pv}$. Because of the fact that α ϵ [0 1], by varying the duty cycle in its definition interval, it is possible to find an optimal value of α designed by α_{opt} for which the output power is maximum for a given voltage V_{pv} and load R_0. To do this with the MPPT technique through the P&O algorithm, it is possible to achieve a variation and fix the duty cycle in order to obtain an optimal output power.

C. *PRINCIPLE OF THE NON-INVERTER BOOST CHOPPER*

Non-inverting buck-boost converter is a configuration of buck converter and boost converter. It allows the voltage to be raised or lowered, while maintaining the sign of the positive output voltage at a chosen reference value [6, 11]. It is represented by Fig. 11:

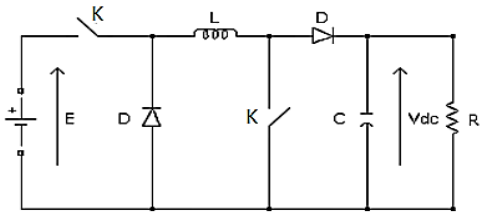

Fig. 11 Diagram of the Buck-Boost chopper

- When the switches *K* are closed during the time interval αT, the functionality of the circuit is described by Eq. (16) :

$$\begin{cases} C\frac{dV_{dc}}{dt} = -\frac{V_{dc}}{R} \\ L\frac{di_L}{dt} = \alpha E \end{cases} \quad (16)$$

- When the switches *K* is opened during the time interval (1-αT), the functionality of the circuit is described by Eq. (17) :

$$\begin{cases} C\frac{dV_{dc}}{dt} = -i_L - \frac{V_{dc}}{R} \\ L\frac{di_L}{dt} = V_{dc} \end{cases} \quad (17)$$

Combining the two functionality intervals, we obtain the global functionality of the electrical circuit described by Eq. (18):

$$\begin{cases} C\frac{dV_{dc}}{dt} = -i_L(1-\alpha) - \frac{V_{dc}}{R} \\ L\frac{di_L}{dt} = \alpha E + V_{dc}(1-\alpha) \end{cases} \quad (18)$$

The application of the state space method of Eq. (16) and Eq. (17) is represented by Eq. (19):

$$\begin{bmatrix} \dot{x}_1 \\ \dot{x}_2 \end{bmatrix} = \begin{bmatrix} 0 & \frac{1-\alpha}{L} \\ \frac{1-\alpha}{C} & -\frac{1}{RC} \end{bmatrix} \begin{bmatrix} x_1 \\ x_2 \end{bmatrix} + \begin{bmatrix} \frac{\alpha}{L} \\ 0 \end{bmatrix} E \quad (19)$$

D. THE SERVO OF NON-INVERTER BUCK-BOOST CHOPPER

To achieve the desired reference voltage, the technique consists in keeping the output voltage of the converter constant. We used a linear control because of its simplicity. Two cascaded proportional integral (PI) correctors were used as shown in Fig.12. The external voltage loop compares the voltage reference value to the measured value and imposes the current reference. The internal current loop compares the current reference value to the actual current value at the converter terminals.

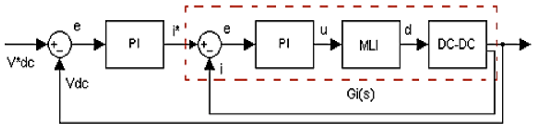

Fig.12 Schematic diagram of the servo-control of the non-inverting Buck-Boost converter

The transfer function equivalent to this servo loop is given by Eq. (20):

$$G(s) = G_{PI}(s) * G_I(s) \quad (20)$$

Where $G_{PI}(s)$ is given by Eq. (21):

$$G_{PI}(s) = K_P + \frac{1}{sT_i} \quad (21)$$

$$G_I(s) = \frac{1}{1+sT}$$

Taking $T_i = RC$ and $T \approx 0.8T_i$, we ave the Eq. (22):

$$G(s) = \frac{\frac{K_P}{T}\left(s+\frac{1}{T_iK_P}\right)}{s^2+s\left(\frac{1+K_P}{T}\right)+\frac{1}{TT_i}} \quad (22)$$

Identifying the second-order characteristic expression given by Eq. (23):

$$s^2 + 2\xi\omega T - 1 \quad (23)$$

Where the coefficient ω is the bandwidth and ξ is the damping coefficient. To have a small overshoot, ξ must be chosen between 0.5 and 0.7.

V. MODELING AND SEARCHING FOR THE MAXIMUM POINT OF POWER POINT

A. SIMULINK MODEL OF PRINCIPLE OF THE NON-INVERTER BOOST CHOPPER

We used the Simulink to model the PV generator using Eq. (7) with:

$$I_{ph} = \frac{G}{Gref}\left(I_{ccref} + K_i(T - T_{ref})\right) \quad (20)$$

And

$$T = T_a + \frac{(NOC-20)}{800} * G \ (21)$$

$$I_s = I_{sref} * \left(\frac{T}{T_{ref}}\right)^{\frac{3}{n}} * \exp\left(q * \frac{E_g}{nK}\left(\frac{1}{T_{ref}} - \frac{1}{T}\right)\right) \ (22)$$

$$I_{sref} = \left(\frac{Iccref + K_i.(T - Tref)}{exp\left(\frac{Vcoref + K_v.(T-Tref)}{nVt}\right) - 1}\right) (23)$$

The Simulink models of I_{ph}, *Is,* and GPV are found in Fig.13a, and 13b, respectively.

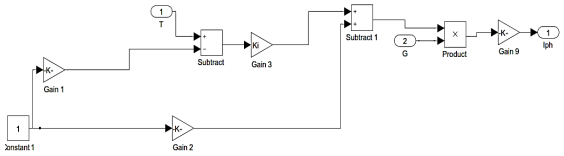

Fig.13a Simulink model of GPV

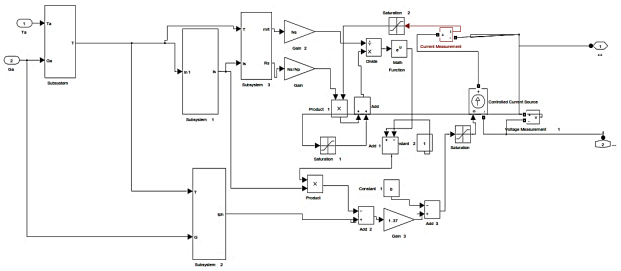

Fig.13b Simulink model of GPV

B. SIMULINK MODEL OF CHOPPERS

B.1. BOOST CHOPPER

We used the boost chopper (voltage booster) as an impedance adapter, allowing to extract the maximum power at the output of the GPV. The modeling that we carried out by the Simulink is represented by Figure 14. It is controlled by the MPPT algorithm.

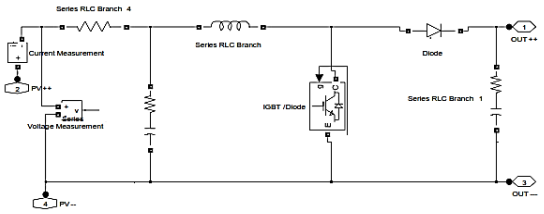

Fig.14 Simulink model of Boost chopper

B.2. NON-INVERTING BUCK-BOOST CHOPPER

We have made the model of the non-inverting buck-boost chopper by Simulink and it is represented in Fig. 15. It is connected to the output of the MPPT regulator, its role is to stabilize the MPPT output DC voltage at a reference value chosen.

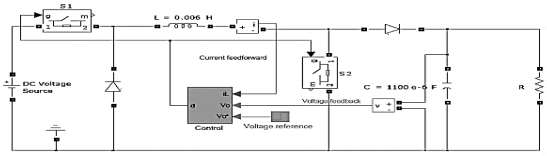

Fig.15 Buck-boost Chopper Simulink Model

C. SIMULINK MODEL OF CHOPPERS

C.1. THE METHOD OF PERTURB AND OBSERVE (P&O)

The MPPT technique through the P&O method consists in creating a disturbance on the voltage of the PV generator while acting on the cyclic ratio α. The power supplied by the PV generator following the disturbance at time *k* is calculated, then it is compared with the previous one at time (*k-1*). If the power increases, the point of maximum power is approached and the variation of the duty cycle is maintained in the same direction. Otherwise, the direction of variation of the duty cycle must be reversed (Fig.16 and Fig.17) [8].

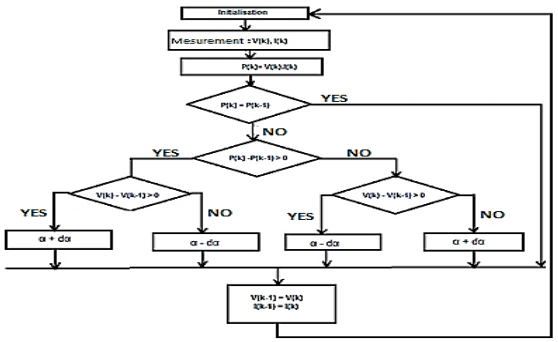

Fig.16 Algorithm of the P&O method

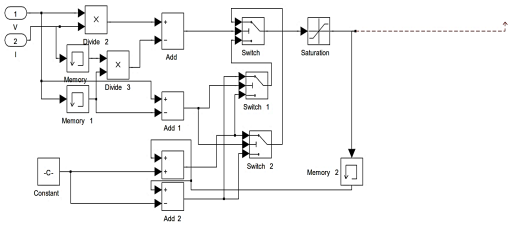

Fig.17 Simulink model of the P&O method algorithm

C.2. NEURO-FUZZY MPPT COMMAND

This command, recently used in the pursuit of the maximum power point, offers the advantage of being robust and does not require exact knowledge of the mathematical model of the system. Moreover, it is better suited for nonlinear systems. The operation of this algorithm is

carried out in three blocks: fuzzification, inference and defuzzification (Fig.18) [7, 9, 13].

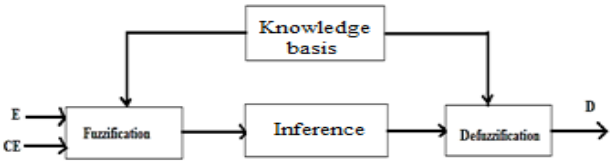

Fig.18 Block diagram of the algorithm based on fuzzy logic

Fuzzification allows the conversion of physical input variables into fuzzy sets, in this case the error *E* and the error variation *CE* are defined Eq. (24) and Eq. (25):

$$E = \frac{P(k)-P(k-1)}{I(k)-I(k-1)} \quad (24)$$

$$CE = E(k) - E(k-1) \quad (25)$$

To these quantities are associated the linguistic variables: NG (Negative Large), NM (Negative Medium), NP (Negative Small), Z (Zero), PP (Positive Small), PM (Positive Medium) and PG (Positive Large). They constitute the input variables of the MPP power management algorithm. Thus, the rules of inference are defined in Table 1 [14, 15].

Table1 Inference rules

CE / E	NG	NM	NP	Z	PP	PM	PG
NG	NG	NG	NG	NM	NM	NP	Z
NM	NG	NG	NM	NM	NP	Z	PP
NP	NG	NM	NM	NP	Z	PP	PM
Z	NM	NM	NP	Z	PP	PM	PM
PP	NM	NP	Z	PP	PM	PM	PG
PM	NP	Z	PP	PM	PM	PG	PG
PG	Z	PP	PM	PM	PG	PG	PG

We carried out the modeling of the fuzzy logic algorithm by the Simulink model. This modeling is represented by Fig.19 a and Fig.19b. So, the input and output variables are the parameters to be configured as indicated in Fig.19.

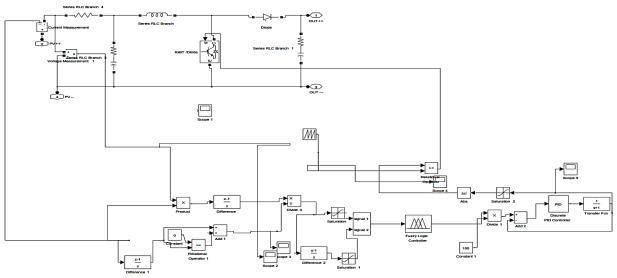

Fig.19a Fuzzy logic algorithm under Simulink/MATLAB environment

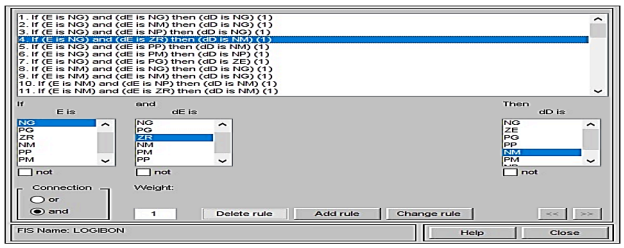

Fig.19b Fuzzy logic algorithm under Simulink/MATLAB environment

Table 2 GPV Electrical Parameters

Photovoltaic Generator		Charge	
Total Power (kW)	11.2	Résistance (Ω)	20
Maximal Power (W)	350	Inductance (H)	-
Voltage Vco (V)	44.5	-	-
Current Icc (A)	10.1	-	-
Photovoltaic module number	32	-	-
Irradiance	500-1000		

VI. RESULTS AND DISCUSSIONS

A. INFLUENCE OF IRRADIANCE ON PHOTOVOLTAIC GENERATOR POWER

We used 32 monocrystalline photovoltaic modules, with a total nominal power of 11.2kW, connected to an RL load. We used two maximum power point tracking techniques: the fuzzy logic algorithm and the Perturb and Observe (P&O) algorithm. The simulation was done by the MATLAB software for 1s duration. The results are presented in Fig.20 and Fig.21.

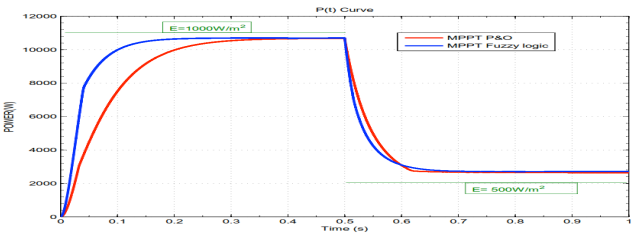

Fig.20 Output power of the GPV+MPPT system obtained thanks to the algorithm of fuzzy logic and P&O

The MPPT algorithm based on fuzzy logic, allowed us to reach 95.1% of maximum power (11.62kW) in 0.18s. However, the P&O algorithm made it possible to reach 95.1% of maximum power in 0.41s. This percentage very close to 100% is linked to the power losses by Joule effect in the electrical devices of the MPPT stage (Fig.20).

In addition, we note that the variation of the irradiance also leads to the variation of the voltage at the output of the generator (Fig.21).

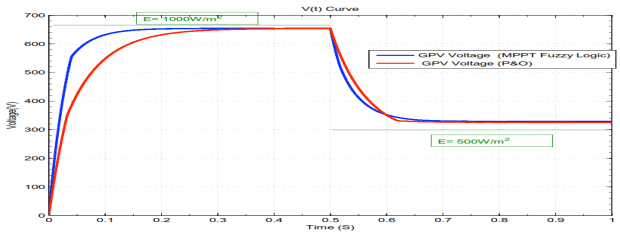

Fig.21 Output voltage of the GPV+MPPT system obtained thanks to the fuzzy logic and P&O algorithm

For an irradiance variation of 1000 to 500W/m^2, this leads to a variation ΔV=324.4V. This variation can cause the inverter to stall. To stabilize the voltage value, we will regulate the DC voltage using the non-inverting Buck-boost chopper.

B. OUTPUT OF THE NON-INVERTING OF THE BUCK-BOOST CHOPPER FOR V_{REF} = 100 VOLT

The Buck-boost chopper is used to regulate the voltage at the output of the GPV+MPPT system. It allows the value of the bus voltage to be fixed at a given reference value. We chose a value V_{ref}=100V, and varied the input voltage. The simulation results allowed us to observe the output voltage according to the variations of the input voltages (Fig.22).

- Case or Ve = 80 V to 160 V

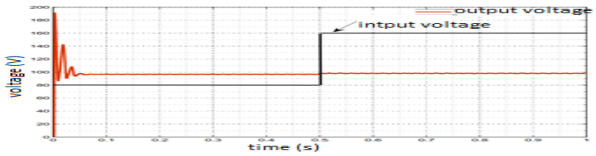

Fig.22 Voltage at the terminals of the Buck-Boost chopper for Ve= 80 V to 160V (Vref=100V)

-Case of Ve = 180V to 90V

In this case, the variation of the input voltage is made from 180V to 90V and the results obtained are shown in Fig.23.

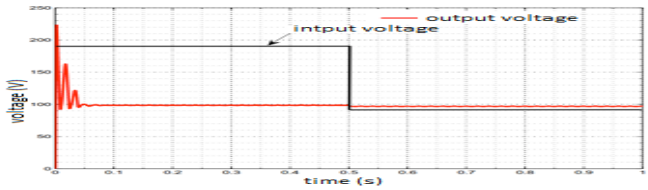

Fig.23 Voltages at the terminals of the Buck-Boost chopper for Ve = 180 to 90 V (V_{ref}=100V)

We can see from Figure 23 that for a variation of input voltage from 80V to 160V and then from 180V to 90V, the output voltage remained constant at 100V. These results confirm the expected theoretical operation.

C. PV GENERATOR AND MPPT OUTPUT VOLTAGE REGULATION

The results in Fig.24 show a strong variation of the alternating voltage of output of the inverter in the case of use of this one without DC bus (curve in blue). In addition, the use of the inverter with the DC bus presents a clear stability of the voltage after the transient state of 0.063s, despite the variation of the solar irradiance from 1000 W/m^2 to 500 W/m^2.

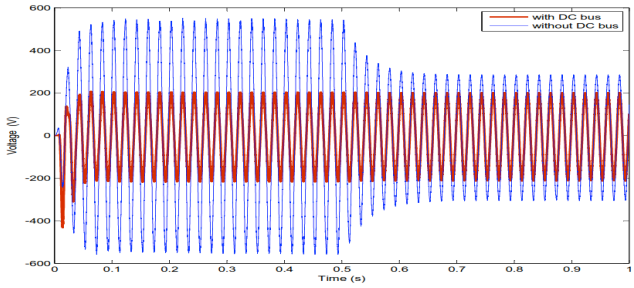

Fig.24 Voltages at the output of the inverter when the irradiance goes from 1000 to 500W/m^2

Finally, a comparative study in the case of use of the inverter with the DC bus is also made through the two techniques of tracking the maximum power point MPPT (Fuzzy Logic and P&O), the results are presented in Fig.25.

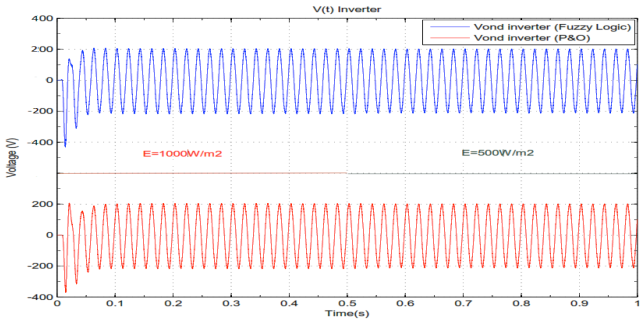

Fig.25 Voltage at the output of the inverter when the irradiance goes from 1000 500W/m^2 to 500W/m^2

We can notice on Fig.25 that with the fuzzy logic MPPT technique, the stability of the ripple voltage is reached at 0.063s and that with the P&O algorithm, this stability is reached at 0.103s. We can conclude that the fuzzy logic MPPT technique allow us to obtain the output voltage stability in order of twice fast than the P&O algorithm; this is very important for the applications that require the fast stability of the voltage for its functionalities.

VII. CONCLUSION

The Sahelian zone is suitable for the exploitation of PV solar energy resources. In particular in Chad, we see an inequitable distribution of solar resources from North to South. Thus, according to the results of data collection in the field and those of NASA for the cities of AMDJARAS and FADA in northern Chad, we may see that these two cities have a solar energy resource significantly higher than that of the city of DOBA in the South.

Given the low efficiency of PV cells, the impedance matching technique through the MPPT algorithm was used to extract the maximum power at the terminals of the PV generator. Among the MPPT algorithms, the P&O method and fuzzy logic have been used. The best performance and the best response were obtained with the fuzzy logic algorithm. However, with the MPPT technique, the output voltage varies greatly.

To improve the stability of the output voltage after the MPPT stage, we used the non-inverting buck-boost chopper. We obtain a very satisfactory result in maintaining the voltage at the reference value, thus solving the problem of voltage dips and inverter dropout in the operating range of the chopper and the inverter. However, this voltage stability is lost when there is no solar power. Thus, as perspectives of this work, we envisage a study of the hybridization of different production techniques on the one hand and on the other hand extend the study to other cities of Chad and especially the remote and isolated areas of the large agglomerations which cannot be reached by the traditional networks of electrical energy of the large productions.

Conflicts of interest We declare that they have no conflict of interest.

References

[1] Tuan TRAN-QUOC and Seddik BACHA, “Coupling photovoltaic inverters and network, control / command aspects and disturbance rejection”, Doctoral Thesis, University of Grenoble, 2012.

[2] Kalmobé Pallaï, “Influence of the Sahelian climate on the yield of photovoltaic cells of different technologies”, Master thesis, University of N'Gaoundéré, 2015.

[3] M. MOUHADJER Samir, “Contribution to the optimization of the yield of photovoltaic and wind generators by integrating electronic adaptation systems with MPPT control”, Doctoral thesis, Abou Bekr Belkaid University of Tlemcen, 2014.

[4] M. Belatel, F. Benchikh, Z. Simohamed, F. Ferhat and F.Z. Aissous, “Technology of the coupling of a hybrid system of the photovoltaic-wind type with the fuel cell for the production of green energy”, Scientific article, Review of Renewable Energies, vol. 14, no. 1, pp.145-162, 2011.

[5] h-Ming Hong, Ting-Chia OU, Kai-Hung Lu, “Development of intelligent MPPT (maximum power point tracking) control for a grid-connected hybrid power generation system”, *Scientific article*, University Sun Yat-Sen de Taiwan. January 2013.

[6] n-Chih Chang, “Applying Robust intelligent algorithm and internet of things to global maximum power point tracking of solar photovoltaic systems”, S*cientific article*, 10 pages, 2020.

[7] Mohammed Faysal Yaden, “Design, production and characterization of a photovoltaic system equipped with digital control and acquisition commands”, S*cientific article*, Mohamed Premier University, July 2013.

[8] Hanen Abbes, Hafedh Abid, Kais Loukil, Ahmad Toumi, Mohamed Abid, “Comparative study of five MPPT control algorithms for a photovoltaic system”, *Scientific article*, University of Tunis, 2013.

[9] Andrianantenaina Tsiory, “Optimization of the energy yield of a photovoltaic system by fuzzy MPPT algorithm”, S*cientific article*, University of Antsiranan.

[10] Mr. Angel Cid Pastor, “Design and production of electronic photovoltaic modules”, *PhD thesis*, National Institute of Applied Sciences of Toulouse, 2006

[11] SIPAROV Dimitar, LAZAROV Vladmir, ROYE Daniel, ZARKOV Zaharie, MANSOURI Oumar, “Modeling of static DC-DC converters for applications in renewable energies using Matlab/simulink”, *Scientific article*, 9 pages, 2009.

[12] Toumi Djaafar, “Comparison of P&O and Fuzzy Logic Controller in MPPT for Photovoltaic (PV) Applications using MATLAB Simulink”, *Scientific article*, 8 pages, 2020.

[13] N. Ould Cherchali, A. Morsli, M. S. Boucherit, L. Barazane, A. Tlemç, “Application of Fuzzy Logic for Tracking the Maximum Power Point of a Photovoltaic System”, *Scientific article,* 6 pages 2022.

[14] Bacem GAIED CHORTANE, “Improvement of the MPPT algorithm for a PV system by integrating new techniques based on artificial intelligence”, *Master’s thesis*, 113 pages, 2022.

[15] Rachida Ghernoug, Maroua Sadallah, Nour El Houda Dhou, “MPPT control by fuzzy logic for photovoltaic systems”, *Master thesis,* 68 pages, 2022.

Kalmobé Pallaï[1*], Mbainaibeye Jérôme[1, 2], Kamta Martin[3], Tom Cherif Bilio[4]

[1] Technology Department, Faculty of Exact and Applied Science, University of N’Djamena, Chad
E-mail: pkalmobe@gmail.com
[2] Faculty of Sciences and Technics, University of Doba, Chad
[3]Ecole Nationale Supérieure Agro-Industrielle (ENSAI), University of N’Gaoundéré
[4] Minister of public function